Analysis of High-Speed Peripheral Jet for ACV Applications

C. D. HOPE-GILL*
Textron's Bell Aerospace Company, Buffalo, N.Y.

With the advent of high-velocity air cushion vehicles with high cushion pressures, a peripheral jet theory is needed that can be accurately applied to compressible peripheral jet flows. An inviscid flow theory is derived, which permits many of the assumptions made in previous theories to be relaxed, yielding results in excellent agreement with the existing incompressible and compressible potential flow peripheral jet theories of Strand and Roche. However, unlike these potential flow analyses, the present method can be extended to real systems with component inefficiencies and flow pressure losses as well as more complex peripheral jet systems. The pressure recovery and nondimensional power coefficient were calculated in terms of the nozzle thickness and angle, jet Mach number, cushion pressure, and clearance height. The results show a substantial decrease in pressure recovery with increasing Mach number and decreasing nozzle flow angle. The optimum or minimum value of the first power coefficient is decreased by approximately 10% as the Mach number is increased from a low subsonic value to unity, which represents an improvement in lifting efficiency. The optimum clearance height to jet thickness ratio is relatively insensitive to Mach number but increases with increasing nozzle angle. For nozzle angles of engineering interest, the optimum height to thickness ratio is approximately two. The heave stability of a vehicle also is improved with increasing Mach number.

Nomenclature

c_p = specific heat at constant pressure
d = kinetic energy to total enthalpy ratio, $(u_b^2/2)/c_pT_T$
h_e = clearance height defined in Fig. 2
$\bar{i}$ = unit vector in horizontal positive direction
l = peripheral jet length
m = mass flow rate
M = Mach number
$\bar{n}$ = unit vector normal (in outward direction) to control surface (Fig. 2)
p = static pressure
P = power
$\mathcal{P}_1$ = first power coefficient (defined in Eq. 19)
$\mathcal{P}_2$ = second power coefficient (defined in Eq. 20)
r_a = radius of curvature of streamlines at nozzle exit
r_1 = radius of curvature of jet's outer streamline at nozzle exit (Fig. 2)
S = control surface area defined in Fig. 2
t = thickness of flow
T = temperature
u = flow velocity
X = $(t_a/h_e)(1 + \sin\theta)$
γ = ratio of specific heats
θ = angle of flow at nozzle exit with respect to vertical
ρ = density

Subscripts

atm = atmospheric conditions
a = nozzle exit flow characteristic
b = ground parallel flow characteristic
c = cushion characteristic at vehicle hard bottom adjacent to nozzle
T = total thermodynamic quantity

1.0 Introduction

THERE is a trend toward higher cushion pressures for air cushion vehicles because it is desirable to reduce the over-all size and structural weight of such vehicles for a given payload. Reducing the vehicle size and weight has the added benefit of decreasing the aerodynamic drag. Two basic lifting systems which produce high positive cushion pressures are illustrated in Fig. 1; they are the plenum chamber and peripheral jet. Peripheral jets were studied herein since they are more efficient. To sustain high cushion pressures by the use of a peripheral jet, the velocity of the jet must be large. It is desirable, therefore, to have a peripheral jet theory available that can be accurately applied to compressible flows.

The importance of using high or near sonic peripheral jet flow velocities can be evaluated by determining the total power required to lift and overcome the momentum drag of a peripheral jet ACV at high speeds. Analytical investigations show that the total power requirement is decreased as the Mach number of the jet is increased.

An inviscid flow theory is derived herein which yields results in excellent agreement with the existing incompressible and compressible potential flow peripheral jet theories of Strand and Roche[2,3] for all clearance heights. Previous inviscid theories for the peripheral jet have used the momentum, and the incompressible Bernoulli equations. This

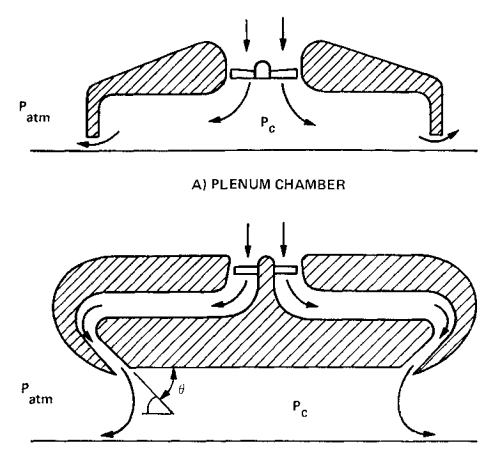

Fig. 1 Air cushion systems.

Received November 26, 1969.
* Research Scientist, Advanced Technology Research Department. Member AIAA.

work has included oversimplifying assumptions such as constant jet thickness[1,4] and constant jet momentum.[5,6] As a result, they are not exact at low vehicle clearance heights[2] or for high-speed compressible jets.

Rather than using the restrictive potential flow theory, it is desirable to incorporate the continuity, momentum and energy equations in an exact analysis since such an analysis could be extended to include viscous effects. Also the inefficiencies and ram pressure losses which occur in real compressor and jet flow ducting systems can be included in this exact analysis of ideal flows.

2.0 Description of Model and Analysis

2.1 Theoretical Model

To illustrate the validity of the general method of analysis presented herein and permit comparison with potential flow theories,[2,3] the following assumptions were made: 1) the perfect gas flow is steady, two-dimensional, inviscid, irrotational and isentropic, 2) the jet flow streamlines are parallel in the immediate region of the jet nozzle exit, and 3) the flow approaches atmospheric pressure when the inviscid jet flow streamlines ultimately become parallel to the ground. This region is denoted by BE in Fig. 2 and is downstream of the initial impingement point of the jet on the ground. In this region, the static pressure across the jet will be uniform and equal to the ambient pressure p_{atm}. Thus, the density and velocity of the flow becomes uniform at BE and, by continuity, the thickness of the jet remains constant thereafter.

2.2 Analysis

The power required to maintain the cushion pressure and the pressure recovery for a compressible peripheral jet will be derived by using the following equations.

2.2.1 Basic equations

1) Integrating the inviscid, two-dimensional momentum equation over the control surface AFGHIC shown in Fig. 2 yields

$$(p_c - p_{atm})\, h_e + p_c t_a \sin\theta - \sin\theta \int_{r_1}^{r_1+t_a} p_a dr_a = \rho_b u_b^2 t_b + \sin\theta \left[\int_{r_1}^{r_1+t_a} \rho_a u_a^2 dr_a\right] \quad (1)$$

2) Equating the local pressure gradient and centrifugal force term across the parallel flow at the nozzle exit, the radial momentum equation at the nozzle exit is

$$\partial p_a/\partial r_a = \rho_a(u_a^2/r_a) \quad (2)$$

3) Equating the mass flow rates through the nozzle and station BE (Fig. 2), the continuity equation is

$$\rho_b u_b t_b = \int_{r_1}^{r_1+t_a} \rho_a u_a\, dr_a \quad (3)$$

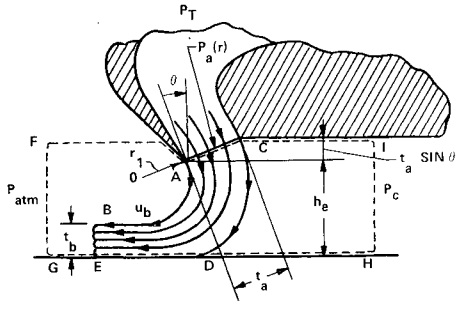

Fig. 2 Control volume for peripheral jet.

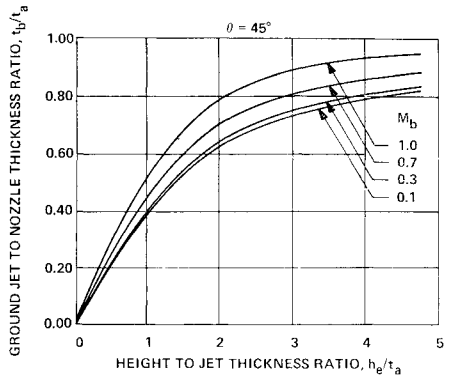

Fig. 3 Variation of jet thickness with Mach numbers.

4) The energy, state, momentum equations, and the irrotational condition for the parallel flow at the exit of the nozzle are, respectively,

$$\tfrac{1}{2}u^2 + c_p T = c_p T_T \quad (4)$$

$$(\rho_T/\rho) = (p_T/p)^{1/\gamma} \quad (5)$$

$$udu + dp/\rho = 0 \quad (6)$$

$$u_b r_1 = u_a r_a \quad (7)$$

2.2.2 Analytical results

Multiplying Eq. (2) by r_a and integrating by parts with respect to r_a along AC, one obtains

$$\int_{r_1}^{r_1+t_a} (p_a + \rho_a u_a^2) dr_a = r_1 p_{atm} \left\{\left(1 + \frac{t_a}{r_1}\right)\frac{p_c}{p_{atm}} - 1\right\} \quad (8)$$

Combining Eqs. (1) and (8) and using the definition,

$$M_b \equiv u_b/(\gamma p_{atm}/\rho_{atm})^{1/2} \quad (9)$$

which applies to isentropically compressed flows,

$$h_e/r_1 = \sin\theta + (t_b/r_1)\gamma M_b^2[1/(p_c - p_{atm})/p_{atm}] \quad (10)$$

Using Eqs. (5), (6), and (7) with the condition that the velocity of the outer jet streamline at atmospheric pressure u_b remains constant and equal to the flow velocity across station BE, Eq. (3) becomes

$$\rho_{atm}\, u_b t_b = \int_{r_1}^{r_1+t_a} \left[\rho_T^{\gamma-1} - \frac{u_b^2 r_1^2}{r_a^2} \times \left(\frac{1}{2}\frac{\rho_T^{\gamma}}{p_T}\frac{\gamma-1}{\gamma}\right)\right]^{1/(\gamma-1)} \frac{u_b r_1}{r_a} dr_a \quad (11)$$

Using Eqs. (5–7) and assuming $\gamma = 1.4$, the following relation is obtained:

$$(t_b/r_1) = (\rho_T/\rho_{atm}) \left\{\frac{1}{5}(1-d)^{5/2} - \frac{1}{5}\left[1 - \frac{d}{(1+t_a/r_1)^2}\right]^{5/2} + \frac{1}{3}(1-d)^{3/2} - \frac{1}{3}\left[1 - \frac{d}{(1+t_a/r_1)^2}\right]^{3/2} + (1-d)^{1/2} - \left[1 - \frac{d}{(1+t_a/r_1)^2}\right]^{3/2} + \frac{1}{2}\ln\left[\frac{(1-d)^{1/2}-1}{(1-d)^{1/2}+1}\,\frac{[1-d/(1+t_a/r_1)^2]^{1/2}+1}{[1-d/(1+t_a/r_1)^2]^{1/2}-1}\right]\right\} \quad (12)$$

where

$$d = (u_b^2/2)/c_p T_T = 1 - T_{atm}/T_T \quad (13)$$

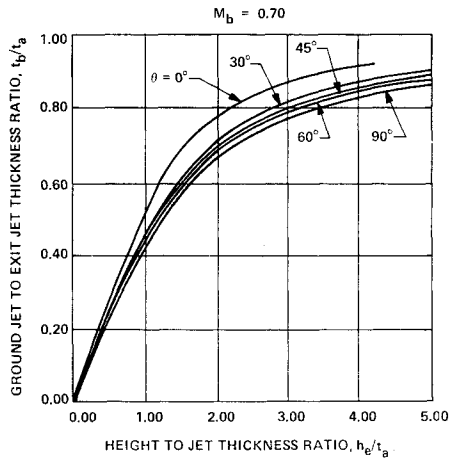

Fig. 4 Variation of ground jet thickness with nozzle angle.

For $d \ll 1$ or $M_b < 0.2$, T_T approaches T_{atm} and ρ_T approaches ρ_{atm} so that Eq. (12) reduces to

$$t_b/r_1 \doteqdot \ln[1 + (t_a/r_1)] \tag{14}$$

Equation (14) is exact for the incompressible flow case.

3.0 Discussion of Results

3.1 Variation of Jet Thickness

Equations (10) and (11) were used to calculate the variation of jet thickness ratio t_b/t_a as a function of h_e/t_a for various flow Mach numbers. Results are presented in Fig. 3. The value of t_b is always less than t_a. Figure 3 shows that the approximation of constant jet thickness improves with increasing height to thickness ratios. This result illustrates why previous analyses[1,4] were inexact at low clearance heights. The incompressible flow equation shows that $t_b \doteqdot t_a$ only for extremely small values of t_a/r_1, which implies large values of h_e/t_a. In addition, Fig. 3 shows that, as M_b approaches unity, the value of t_b/t_a approaches unity more quickly as h_e/t_a increases.

Figure 4 shows that the ground jet to nozzle thickness ratio t_b/t_a decreases with increasing values of θ for a given M_b and h_e/t_a. The value of t_b/t_a approaches unity more quickly for smaller values of θ.

3.2 First and Second Power Coefficients

3.2.1 Discussion of power coefficients

For the case where the ACV is stationary (no ram pressure recovery) and the compression and ducting processes are

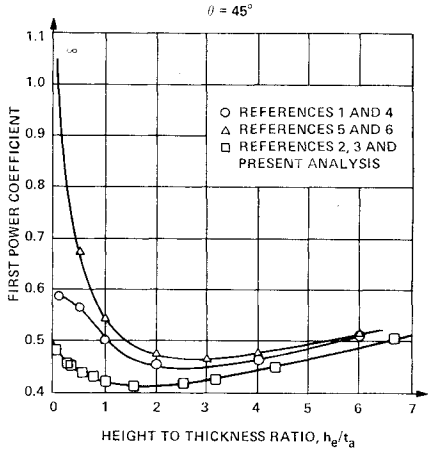

Fig. 5 Comparison of incompressible jet theories.

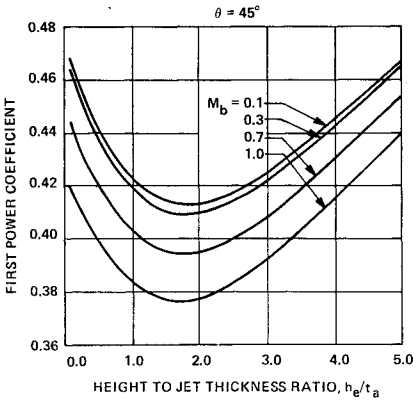

Fig. 6 Variation of first power coefficient for various Mach numbers.

assumed isentropic, the power requirement can be expressed as

$$P = mc_p(T_T - T_{atm}) = l t_b u_b p_{atm}(\gamma/\gamma - 1)[(p_T/p_{atm})^{(\gamma-1)/\gamma} - 1] \tag{15}$$

The power can be calculated in terms of h_e/t_a, θ, and M_b by using Eqs. (4), (5), (10), and (12). It is convenient to define a first power coefficient as

$$\mathcal{P}_1 \equiv \frac{P}{(2/\rho_{atm})^{1/2}(p_c - p_{atm})^{3/2} l h_e} = \left\{\left(\frac{\gamma}{\gamma-1}\right)\left(\left[\frac{p_T}{p_{atm}}\right]^{(\gamma-1)/\gamma} - 1\right)[1/(p_c - p_{atm})/p_{atm}]\right\}^{3/2}\left(\frac{t_b}{h_e}\right) \tag{16}$$

The first power coefficient has practical meaning since, once the required design clearance height and cushion pressure p_c are designated, the first power coefficient can be used to determine the optimum nozzle thickness for a given M_b and θ.

For the incompressible flow case, the denominator of $\mathcal{P}_1$ expresses the power expended in replenishing the air supplied to a static plenum chamber having a clearance height h_e and p_c equal to p_T. Thus, for incompressible flows, $\mathcal{P}_1$ is the ratio of the power requirement of a peripheral jet lifting system to the power requirement of an ideal plenum chamber system.

When the nozzle thickness and angle is predetermined or constant and the height is variable, the second nondimensional power coefficient defined below is useful for considering the power requirements associated with an existing peripheral jet system.

$$\mathcal{P}_2 = \frac{P}{(2/\rho_{atm})^{1/2}(p_c - p_{atm})^{3/2} l t_a} = \mathcal{P}_1\left(\frac{h_e}{t_a}\right) \tag{17}$$

Both nondimensional power coefficients can be obtained for any given values of θ, M_b, and h_e/t_a.

By rearranging the nondimensional terms of Strand's report, and the incompressible flow results of Roche's report,[3] a comparison can be made based on $\mathcal{P}_1$. Agreement with the results of this report was extremely good at all heights, and consequently $\mathcal{P}_1$, for both the potential theory and the theory presented herein, can be represented in Fig. 5 by a single curve.

While deriving the peripheral jet power requirements, the authors of other reports have assumed that either the thickness of the jet remained constant[1,4] or the jet momen-

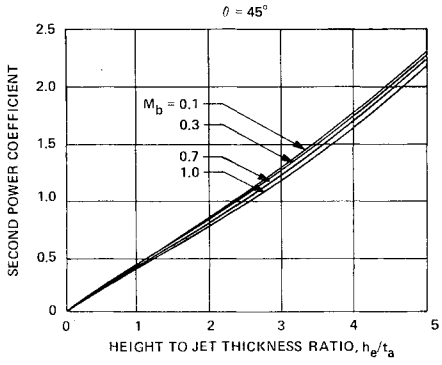

Fig. 7 Variation of second power coefficient.

tum remained constant[5,6] in place of using the continuity equation. Instead of employing a momentum control volume, it has often been assumed that the radius of curvature of the peripheral jet also remained constant.[1,4]

If the assumptions of constant jet thickness and radius of curvature are used, the first power coefficient for incompressible flows becomes

$$\mathcal{P}_1 = \frac{P}{(2/\rho)^{1/2}(p_c - p_{atm})^{3/2} l h_e} = \frac{(1 - e^{-X})}{(1 - e^{-2X})^{3/2}(1 + \sin\theta)} \quad (18)$$

when an irrotational velocity profile is assumed at the exit of the nozzle. For this case, the minimum value of the first power coefficient occurs for $h_e/t_a = 2.44$ (see Ref. 1) as shown in Fig. 5.

For the present analysis of the incompressible flow case, when $\theta = 45°$, the minimum point of the first power coefficient shown in Fig. 5 occurs at $h_e/t_a = 1.8$.

On the basis of the theory derived herein, it would appear that, to optimize the power input for a given value of h_e, the nozzle should be designed so that it is slightly greater than one-half h_e. According to Eq. (18), the nozzle thickness should be less than a half h_e for a nozzle angle of 45°.

3.2.2 *Effect of jet mach number on power coefficients*

The variation of the first nondimensional power coefficient with h_e/t_a is shown in Fig. 6 for $\theta = 45°$. The value of $\mathcal{P}_1$ at a given value of h_e/t_a decreases rapidly with Mach number. In the region where $h_e/t_a \approx 2$, there is approximately a 10% decrease in the power coefficient as M_b increases from 0.1 to 1.0. The optimum value of h_e/t_a remains between 1.5 and 2 for all M_b considered. Figure 6 shows that slightly thicker jets are desirable at higher M_b. The curves in Fig. 6, being relatively flat for h_e/t_a between 1.2 and 2.4, show that there is some latitude in the choice of the optimum height to thickness ratio.

For given values of h_e, t_a, and M_b, the power requirement P increases as the product of $(p_c - p_{atm})^{3/2}$ and $\mathcal{P}_1$ (Eq. 16). Since, for a given value of P_c, h_e, and t_a, $\mathcal{P}_1$ is decreased by 10% as M_b is increased from a small value to unity, the variation of the power requirement is also decreased by 10%.

Figure 7 shows the variation of $\mathcal{P}_2$ with h_e/t_a. Since, at a height to thickness ratio between 1 and 3, $\mathcal{P}_1$ is reduced by over 10% as M_b is increased to unity, Fig. 7 and Eq. 17 show that $\mathcal{P}_2$ is also decreased by over 10%. The second power coefficient curves shown in Fig. 7 show the effect of flow compressibility or Mach number for the case when t_a and p_c are predetermined while h_e and P_T are varied.

A heave stability characteristic is indicated by the slope of $\mathcal{P}_2$ with h_e/t_a. This characteristic is defined as the partial differential of the power requirement with clearance height for constant values of p_c and $(\partial P/\partial h_e)_{p_c}$. The stability of a vehicle undergoing heave motion is improved as the slope of $\mathcal{P}_2$ is decreased since the decrease means that the power requirement is less dependent on the variations of h_e. As

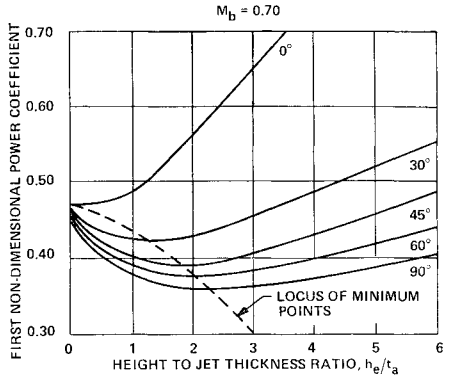

Fig. 8 Variation of first power coefficient with nozzle angle.

shown by Fig. 7, the stability of the vehicle is improved for higher M_b.

3.2.3 *Effect of flow angle on power coefficients*

Figure 8 illustrates the necessity of having θ greater than zero in order that the minimum value of $\mathcal{P}_1$ exists at $h_e/t_a > 0$. As θ is increased, the optimum design h_e/t_a increases from zero to approximately two. By increasing θ from 0° to 30°, the power required to maintain a given cushion pressure is decreased by 25% at $h_e/t_a = 2$ for $M_b = 0.7$. As indicated in Figs. 8 and 9, under the ideal flow conditions assumed herein, it is desirable to have θ equal to at least 60°. However, in actual peripheral jet systems, there is an increased total pressure loss as the flow angle is increased caused by viscous and turning effects. By increasing θ to a value greater than 60°, the loss in total pressure will become large enough to cause a net decrease in over-all performance. Consequently, practical peripheral jet systems have a value of θ in the region of 30° to 45°. For the analyses presented herein, a practical value of $\theta = 45°$ has been used.

3.3 Pressure Recovery

3.3.1 *Comparison of theoretical results*

By integrating Eq. (6) across the jet flow at the nozzle's exit, using Eqs. (5) and (7), the pressure recovery may be expressed as

$$\frac{p_c - p_{atm}}{p_T - p_{atm}} = \frac{1}{(p_T/p_{atm} - 1)}\left(\left\{\frac{1}{(1 + t_a/r_1)^2} + \frac{p_T}{p_{atm}}^{(\gamma-1)/\gamma}\left[1 - \frac{1}{(1 + t_a/r_1)^2}\right]\right\}^{\gamma/(\gamma-1)} - 1\right) \quad (19)$$

The relationship between M_b, γ, and p_T/p_{atm} can be obtained from Eq. (4) and the perfect gas law equation. The

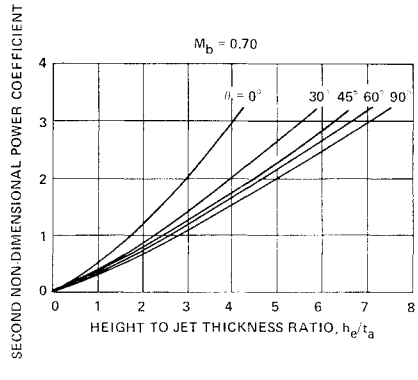

Fig. 9 Variation of second power coefficient with nozzle angle.

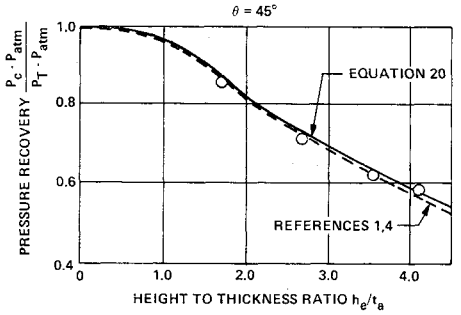

Fig. 10 Pressure recovery for incompressible flows.

incompressible flow pressure relationship, derived from Eqs. (7) and either (2) or (6), is

$$(p_c - p_{atm})/(p_T - p_{atm}) = 1 - 1/(1 + t_{a_1}/r_1)^2 \quad (20)$$

A well-accepted incompressible flow equation for the cushion pressure recovery associated with the assumptions of Eq. (18) is[1,4]

$$(p_c - p_{atm})/(p_T - p_{atm}) = 1 - \exp[-(2t_a/h_e)(1 + \sin\theta)] \quad (21)$$

Equations (20) and (21) agree for small values of t_a/r_1 since

$$h_e/r_1 \doteq (1 + \sin\theta)(1 + t_a/r_1) \quad (22)$$

for small t_a/r_1 or large h_e/t_a. The theoretical pressure recovery curves corresponding to Eqs. (20) and (21) are plotted in Fig. 10 and are in good agreement.

3.3.2 Effect of mach number on pressure recovery

As shown in Fig. 11, the pressure recovery decreases with increasing Mach number. As the velocity of the jet increases from a low subsonic value to sonic velocity, there is an approximate decrease in pressure recovery of 2% and 10% at $h_e/t_a = 2$ and 4, respectively.

3.3.3 Effect of flow angle on pressure recovery

As shown in Fig. 12, pressure recovery is highly sensitive to θ. The decrease in pressure recovery is significant for θ between $\theta = 30°$ and 0°. At $h_e/t_a = 4$, Fig. 12 indicates a pressure recovery reduction of 10% as θ is decreased from 30° to 15°.

3.3.4 Comparison of experimental and theoretical results

The applicability to engineering purposes of previous theories and the present theory depends in a large part on the disparity between the pressure recovery achieved under actual operating conditions and the theoretically predicted pressure recovery.

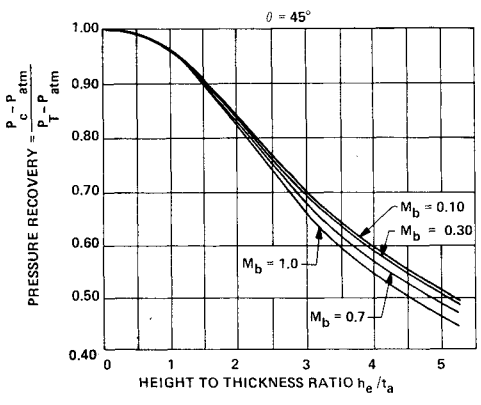

Fig. 11 Cushion pressure recovery for compressible flows.

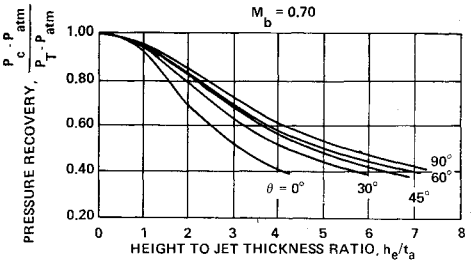

Fig. 12 Variation of pressure recovery with nozzle angle.

Mair[1] presents experimental data in excellent agreement with Eq. (20). Data[1] are presented in Fig. 10 for nozzle thicknesses greater than 0.4 in. However, at $h_e/t_a = 4$, the experimental results of Richardson[7] differ as much as 40% from the pressure recovery predicted by Eqs. (20) and (21). Richardson found that for relatively low-velocity jets and thin nozzles (0.1 in.), giving low Reynolds numbers, $\sim 10^4$, the discrepancy between the theoretical pressure recovery curve and the experimental results was far greater than for thicker nozzles (0.2 in.) and higher flow velocities and Reynolds numbers, $\sim 10^5$. From Mair's data, it would appear that a significant portion of the discrepancy can be explained by taking into account 1) the boundary-layer displacement thickness along the walls of the jet nozzle and the ground surface, 2) the Mach number or flow compressibility effect, and 3) the actual flow angles at a peripheral jet nozzle exit which may be far less than the designed flow angles. The boundary-layer displacement thickness reduces the effective value of t_a, and consequently, raises the effective height to thickness ratio. If the latter ratio was used as the height to thickness ratio, the difference between the ideal and actual pressure recovery curves would be reduced. The Mach number effect is described in Sec. 3.2.2. Since the actual flow angle of a 30° nozzle of the type used by Richardson et al.[7] approaches 15°, the flow angle effect described in Sec. 3.2.3 cannot be discounted.

4.0 Extension of Present Theory

Because of the inefficiencies in the system, the static temperature of the nozzle jet flow is increased above T_{atm}. By including this effect in a more practical but complex theoretical derivation, a more accurate evaluation of real peripheral jet characteristics can be made. By using the potential flow theory of Strand[2] and Roche,[3] one is restricted to the analysis of inviscid, irrotational flows. Using the general method discussed herein, complex peripheral jet systems can also be analyzed. Such analyses are currently in progress.

5.0 Conclusions

1) The ratio t_b/t_a can take on any value between zero and unity. Increasing M_b and decreasing θ causes an increase in t_b/t_a. 2) The compressibility effect is beneficial to the lifting efficiency as indicated by an approximate 10% decrease in the power coefficients as the jet Mach number is increased from zero to unity at $h_e/t_a = 2$. 3) Results indicate that under static conditions the design clearance height should not be greater than twice the nozzle thickness. There is only a slight decrease in the optimum value of h_e/t_a as the Mach number is increased to unity. 4) The nozzle thickness required to optimize the power requirements for a given clearance height increases with decreasing values of θ. 5) The heave stability characteristic improves with increasing jet Mach number. 6) The pressure recovery of a peripheral jet decreases with increasing Mach number. 7) The pressure recovery of peripheral jet is greatly affected by the nozzle flow angle. In evaluating a peripheral jet system, it is important to realize the difference between the design and

actual flow angles. 8) The analysis presented herein agrees with the potential flow theories of Strand[2] and Roche[3] for all height to thickness ratios. 9) Unlike potential flow theories which are restricted to irrotational, inviscid flow analyses, this general method of analysis provides the basis for an accurate evaluation of the performance characteristics of compressible flow peripheral jets wi h viscous effects. Furthermore, this method of analysis may be extended to analyze more complex peripheral jet systems.

6.0 References

[1] Mair, W. A., "The Physical Principles of Hovercraft," *Journal of the Royal Aeronautical Society*, Oct. 1964, pp. 683–695.

[2] Strand, T., "Inviscid, Incompressible Flow Theory of Static Peripheral Jets in Proximity to Ground," *Journal of Aerospace Sciences*, Vol. 28, No. 1, Jan. 1961, pp. 27–33.

[3] Roche, D. J. T., "The Peripheral Jet Theory," Proceedings of the 115th International Congress, Munich, Aug. 30–Sept. 5, 1964, pp. 685–695.

[4] Stanton-Jones, R., "The Development of the Saunders-Roe Hovercraft SRN 1," Symposium on Ground Effect Phenomena (Saunders-Roe Rept. T.P. 414), Oct. 1959, Princeton University.

[5] Richardson, H. H. and Captain, K. M., "Simplified Static Performance Characteristics of Low Pressure Plenum and Peripheral Jet Fluid Suspensions," Jan. 1968, Dept. of Mechanical Engineering, Engineering Projects Lab., Massachusetts Institute of Technology.

[6] West, A. A., "The Compressible Hovercraft Jet," *The Aeronautical Quarterly*, Nov. 1968, pp. 317–326.

[7] Richardson, H. H., Ribich, W. A., and Ercan, Y., "Pressure-Flow-Displacement Characteristics of a Peripheral Jet Fluid Suspension," Rept. DSR 76110-7, Clearinghouse No. PB 176 138, June 1, 1968.